

Simultaneous detection of microcystin-LR and okadaic acid using a dual fluorescence resonance energy transfer aptasensor

Shijia Wu · Nuo Duan · Hui Zhang · Zhouping Wang

Received: 22 October 2014 / Revised: 23 November 2014 / Accepted: 27 November 2014 / Published online: 10 December 2014
© Springer-Verlag Berlin Heidelberg 2014

Abstract Algal toxins can cause neurovirulence, hepatotoxicity, and cytotoxicity in humans through the consumption of contaminated water and food. In this work, we presented a novel aptasensor for the simultaneous detection of two algal toxins, microcystin-LR (MC-LR) and okadaic acid (OA). This system employed green and red upconversion nanoparticle (UCNP) luminescence as the donors and two quenchers (BHQ₁ and BHQ₃) as the corresponding acceptors. The two donor–acceptor couples were fabricated by hybridizing the aptamers with their corresponding complementary DNA. The results indicated that the green and red upconversion luminescence could be quenched by the quencher probes because of their highly overlapping spectrum. In the presence of MC-LR and OA, the aptamers preferred to bind to their corresponding analytes and de-hybridize with the complementary DNA. This effect became sufficiently large to prevent green and red luminescence quenching. Under the optimized experimental conditions, the relative luminescence intensity increased as the algal toxin concentrations increased, allowing for the quantification of MC-LR and OA. The relationships between the luminescence intensity and plotting logarithms of algal toxin concentrations were linear in the range from 0.1 to 50 ng mL⁻¹ for MC-LR and OA. As a practical application, this type of dual fluorescence resonance energy transfer (FRET) aptasensor was used to monitor the MC-LR and OA

levels in naturally contaminated food samples such as fish and shrimps.

Keywords Upconversion nanoparticles · Microcystin-LR · Okadaic acid · Aptamer · Simultaneous detection

Introduction

Cyanobacteria (formerly known as blue–green algae) have been found in both freshwater and marine environments and produce neurotoxins, hepatotoxins, and cytotoxins [1]. Among all toxins, microcystin-LR (MC-LR) and okadaic acid (OA) are of paramount importance and are considered the hepatotoxins with the largest distribution. Human beings are most likely to be exposed to MC-LR and OA through the consumption of contaminated drinking water or recreational activities such as swimming. Moreover, an additional exposure route may be through the consumption of contaminated foods. For example, these toxins have been shown to accumulate in certain species of freshwater mussel. Both MC-LR and OA have been shown to cause tumor promotion and immunotoxic effects [2, 3]. The toxicity of MC-LR and OA is assumed to be due to the inhibition of protein phosphatases 1 and 2A (PP1 and PP2A) [4, 5], two key enzymes in cellular processes. The contamination of shellfish with MC-LR and OA has harmful impacts on both human health and the shellfish industry worldwide; as a result, detection methods for MC-LR and OA are being developed. The general detection methods include high-performance liquid chromatography (HPLC) [6, 7], mass spectrometry [8, 9], immunoassays [10–12], and mouse bioassays (MBA) [13]. Of these methods, chromatography detection methods require expensive equipment and highly qualified personnel due to the high variability of toxin structures. Chromatography detection methods also suffer from the complexity of pretreatment of the collected

S. Wu · N. Duan (✉) · Z. Wang (✉)
State Key Laboratory of Food Science and Technology, School of Food Science and Technology, Synergetic Innovation Center of Food Safety and Nutrition, Jiangnan University, Wuxi 214122, China
e-mail: never_good_love@126.com
e-mail: wangzp1974@hotmail.com

H. Zhang
China Rural Technology Development Center, Beijing 100045, China

samples as well as the long analysis time. Mouse bioassays lack sensitivity and selectivity. Immunoassays are simple but time consuming. Currently, the high cost of the antibodies, limited stability, and special storage conditions remain challenges for the adoption of immunosensor technologies.

In the past decade, the rapid development of nanotechnology has attracted significant attention to the extraordinary biological features of nanomaterials. Due to their unique physical and chemical properties, nanomaterials are playing an increasingly important role in the improvement of biosensing. There has been considerable interest in rare-earth upconversion nanoparticles (UCNPs) that are doped with lanthanide ions. Lanthanide-doped near-infrared (NIR)-to-visible UCNPs are capable of emitting strong visible luminescence with the excitation of NIR light (typically 980 nm) [14]. UCNPs have significant advantages over the traditional organic fluorophores as fluorescent biolabels because of their attractive optical and chemical features, their lack of autofluorescence, and the fact that a light-scattering background can be induced by biological samples [15, 16]. As a result, the signal-to-background ratio can be greatly improved. In addition, UCNPs have also attracted increasing interest because of their tunable optical properties, which are tunable through varying their lanthanide dopants including Er^{3+} , Tm^{3+} , and Ho^{3+} [17, 18]. Some multicolor UCNP-based biosensors were successfully built in our group [19–23]. Those works helped us develop the novel biosensors for the simultaneous detection of various analytes.

Herein, NaYF_4 : Yb, Ho UCNPs and Mn^{2+} -doped NaYF_4 : Yb, Er UCNPs were used as donors when excited by a 980-nm laser. As potential alternatives, BHQ_1 and BHQ_3 were chosen as the acceptors for the corresponding donors because of their good quenching abilities and specific absorption. As a result, a homogenous dual fluorescence resonance energy transfer (FRET) system was fabricated between two donor–acceptor pairs to detect MC-LR and OA simultaneously. The presented method here is highly sensitive and selective due to the near-infrared laser-induced upconversion luminescence without autofluorescence interference and the high specificity of the aptamers. More importantly, two colors of UCNPs were used as donors and two different quencher dyes were used as acceptors in the homogenous system, which has potential for future application.

Materials and methods

Materials and apparatus

MnCl_2 , NaF, NaOH, HCl, toluene, cyclohexane, and ethanol were of analytical grade. All of these chemicals above were purchased from Sinopharm Chemical Reagent Co., Ltd. (Shanghai, China). 1-Ethyl-3-(3-dimethylaminopropyl)

carbodiimide hydrochloride (EDC), *N*-hydroxysulfosuccinimide sodium salt (sulfo-NHS), poly (acrylic acid) (PAA), diethylene glycol (DEG), and oleic acid were obtained from Sigma-Aldrich (USA). The rare-earth nitrates including $\text{Y}(\text{NO}_3)_3 \cdot 6\text{H}_2\text{O}$, $\text{Yb}(\text{NO}_3)_3 \cdot 5\text{H}_2\text{O}$, $\text{Ho}(\text{NO}_3)_3 \cdot 5\text{H}_2\text{O}$, and $\text{Er}(\text{NO}_3)_3 \cdot 5\text{H}_2\text{O}$ were 99.99 % pure and purchased from Aladdin Industrial Inc. (Shanghai, China). The sequences of the MC-LR aptamer [24] and the OA aptamer [25] (in Table 1) were synthesized by Sangon Biotechnology Co., Ltd. (Shanghai, China). The complementary DNA of the MC-LR aptamer and the complementary DNA of the OA aptamer (in Table 1) were synthesized by TaKaRa Biotechnology Co., Ltd. (Dalian, China). The standard solution of MC-LR and OA was purchased from Taileqi Technology Co., Ltd. (Beijing, China).

The UCNPs were characterized by a transmission electron microscope (TEM, JEM-2100HR) with an operating voltage of 200 kV (JEOL Ltd., Japan). Upconversion luminescence spectra were taken using an F-7000 luminescence spectrophotometer (Hitachi Co., Japan) equipped with an external 980-nm laser (Hi-Tech Optoelectronic Co., Ltd., Beijing, China). UV–visible absorption spectra were measured using a UV-1800 spectrophotometer (Shimadzu, Japan). Fourier transform infrared (FT-IR) was recorded on a Nicolet Nexus 470 Fourier transform infrared spectrophotometer (Thermo Electron Co., USA). Ultrapure water of resistivity $18.2 \text{ M}\Omega \text{ cm}^{-1}$ was obtained from a Milli-Q Water System (Millipore Corp., Bedford, MA, USA) and was used throughout for the preparation of solutions.

Synthesis of hydrophobic oleic acid-capped UCNPs

The NaYF_4 : Yb, Ho UCNPs were synthesized following a previously reported protocol with some modification [26]. Basically, NaOH (0.3 g), deionized water (1.5 mL), oleic acid (5 mL), and ethanol (10 mL) were mixed under agitation to form a homogeneous solution. Then, 0.936 mL of 0.5 M $\text{Y}(\text{NO}_3)_3$, 0.6 mL of 0.2 M $\text{Yb}(\text{NO}_3)_3$, and 0.06 mL of 0.2 M $\text{Ho}(\text{NO}_3)_3$ (Y:Yb:Ho=78:20:2 mol%) were added to the above mixture and stirred thoroughly. The NaYF_4 : Yb, Er/Mn UCNP synthesis procedure was as follows: 0.6 mL of 0.5 mol L^{-1} MnCl_2 , 1 mL of 0.5 mol L^{-1} $\text{Y}(\text{NO}_3)_3$, 0.9 mL of 0.2 mol L^{-1} $\text{Yb}(\text{NO}_3)_3$, and 0.1 mL of 0.2 mol L^{-1} $\text{Er}(\text{NO}_3)_3$ (Mn:Y:Yb:Er=30:50:18:2 mol%) were added to the mixture and stirred thoroughly. A solution containing 4 mmol of NaF in 4 mL of deionized water was added dropwise to the mixture. After vigorous stirring at room temperature for 15 min, the colloidal solution was transferred to a 50-mL Teflon-lined autoclave, sealed, and heated at 195 °C for 12 h. Then, the solution was cooled to room temperature, and the UCNPs were precipitated by centrifugation. Later on, the oleic acid-capped UCNPs were washed three times with ethanol.

Table 1 The sequences of the MC-LR aptamers and the OA aptamer and the complementary DNA of the MC-LR aptamer and OA aptamers

Name	Abbreviation	Sequence (5'–3')
MC-LR aptamer	Apt ₁	bio-GGCGCCAAACAGGACCACCATGACAATTACCC ATACCA CCTCATTATGCCCCATCTCCGC
Complementary DNA of the MC-LR aptamer	cDNA ₁	AATGAGGTGGTATGGGTAATTGTCATGGTGGTCTGTTTGG-BHQ ₃
OA aptamer	Apt ₂	bio-GGTCACCAACAACAGGGAGCGCTACGCGAAGGGT CAAT GTGACGTCATGCGGATGTGTGG
Complementary DNA of the OA aptamer	cDNA ₂	TCGTCACATTGACCCCTTCGCGTAGCGCTCCCTGTTGTTGG-BHQ ₁

Synthesis of hydrophilic PAA-capped UCNPs

The above hydrophobic UCNPs were converted to aqueous phase by a surface ligand-exchange strategy [27]. Typically, PAA (0.5 g) was added to 10 mL of DEG, and the mixture was heated to 110 °C with vigorous stirring under nitrogen for 15 min. A toluene solution of the oleic acid-capped UCNPs (50 mg in 2 mL) was quickly injected into the hot solution and allowed to evaporate for 15 min. Then, the system was heated to 240 °C for 2 h and refluxed under nitrogen. The reaction mixture was cooled to room temperature. A dilute hydrochloric aqueous solution was added in excess to the reaction mixture, which was then stirred for 30 min. A white powder was obtained via centrifugation and washed three times with pure water. The prepared PAA-capped UCNP powder was well dispersed in water and aqueous buffer.

Preparation of aptamer-functionalized UCNPs

For example, in the case of NaYF₄: Yb, Ho UCNPs conjugated with biotinylated Apt₁, 5 mg of PAA-capped UCNPs was first dispersed in 5 mL of 10 mM phosphate-buffered saline (PBS) solution at pH 7.4, and 0.4 mL of EDC (2 mg mL⁻¹) and 0.2 mL of NHS (2 mg mL⁻¹) were subsequently introduced into the solution. The reaction was continued for 2 h at 37 °C in a reciprocating oscillator. After incubation, the UCNPs were separated by centrifugation and washed three times with PBS. Next, the activated UCNPs were dispersed in 5 mL of PBS solution and 200 µL of 5.0 mg mL⁻¹ avidin was subsequently added. The mixture was then incubated at 37 °C with oscillation for another 2 h. After removal of the supernatant, the avidin-conjugated UCNPs were washed twice with PBS by centrifugation separation and then finally redispersed in fresh PBS. Finally, biotinylated Apt₁ was immobilized on avidin-conjugated UCNPs through a biotin–avidin affinity reaction. NaYF₄: Yb, Er/Mn UCNPs conjugated with biotinylated Apt₂ were prepared using a similar protocol.

Simultaneous detection of MC-LR and OA

The luminescent bioassay platform for the simultaneous detection of MC-LR and OA based on the dual FRET analysis

was performed according to the following steps. First, 200 µL of Apt₁-functionalized NaYF₄: Yb, Ho UCNPs and Apt₂-functionalized NaYF₄: Yb, Er/Mn UCNPs were mixed, and specific amounts of MC-LR and OA standard solutions were added. The mixture was incubated at room temperature for 30 min. During the incubation, MC-LR was recognized and bound by Apt₁-functionalized NaYF₄: Yb, Ho UCNPs, and OA was recognized and bound by Apt₂-functionalized NaYF₄: Yb, Er/Mn UCNPs. Subsequently, two quencher probes, 100 µL of cDNA₁-BHQ₁ and 100 µL of cDNA₂-BHQ₃ were added to the mixture solution, which was further incubated at 37 °C for 50 min. The upconversion luminescence spectra of the final mixture were then measured using an F-7000 luminescence spectrometer with an external 980-nm laser as the excitation source in place of the xenon lamp in the spectrometer. Slits for both the excitation and the emission were set at 5 nm.

Real sample preparation and measurement

Water samples were from Tai Lake and tap water. The water was left to stand for 30 min to precipitate macroaggregates and seston. The supernatant was subsequently filtered through a 0.45-µm filtration membrane. Fresh shrimps and fish were purchased from a local supermarket and transported to the laboratory in containers with ice bags. Prior to use for testing, 25 g shrimps or fish was aseptically dipped in 225 mL PBS pH 7.4 and homogenized for 5 min, followed by filtering to remove large debris. The real food and spiked samples were then analyzed using the method described previously and measured.

Results and discussion

Principle of dual FRET simultaneous detection for MC-LR and OA

The assay protocol for simultaneously detecting MC-LR and OA using the dual FRET system based on two couples of donors–acceptors was depicted schematically in Fig. 1. The

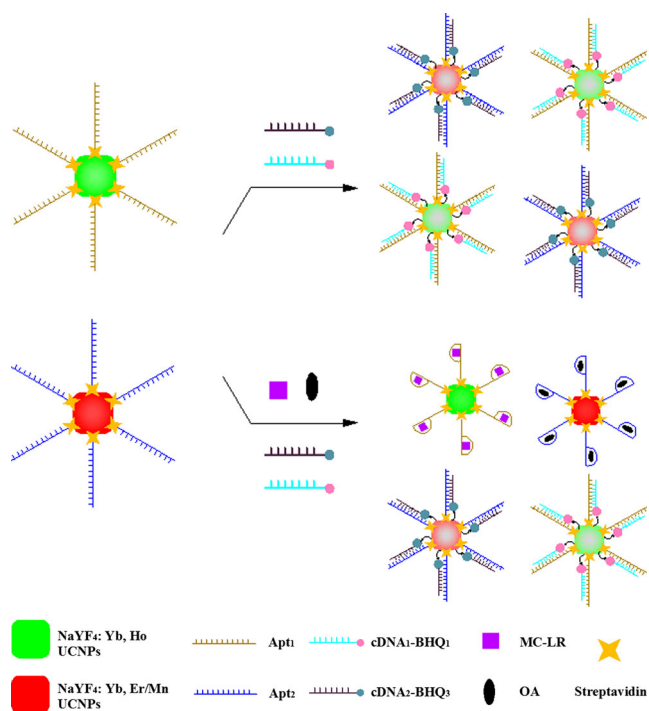


Fig. 1 Schematic illustration of the dual FRET aptasensor between the upconversion nanoparticles and quenching agent for the simultaneous detection of MC-LR and OA

biotinylated-modified aptamers were attached to the avidin-functionalized UCNPs based on the biotin–avidin affinity reaction. In the absence of MC-LR and OA, the dual FRET system was established between two donor–acceptor couples: Apt₁-functionalized NaYF₄: Yb, Ho UCNPs hybridized with cDNA₁-BHQ₁ and Apt₂-functionalized NaYF₄: Yb, Er/Mn UCNPs hybridized with cDNA₂-BHQ₃. Thus, the energy donors and acceptors were placed in close proximity, and the green and red upconversion luminescence could be quenched by quencher probes because of their highly overlapped spectra. In the presence of MC-LR and OA, the aptamers preferred to bind to their corresponding analytes, which led to a change in the aptamer conformations. The complexes of aptamers–analytes could not hybridize with their corresponding complementary DNA. This effect became sufficiently large to prevent luminescence quenching. As a result, with the increased concentrations of MC-LR and OA, a gradual increase of the upconversion luminescence signals was observed. More importantly, the two donor–acceptor couples were independent and did not interfere with each other because each complementary DNA was specially designed to match the corresponding aptamers and the upconversion luminescence of two types of UCNPs was distinguishable.

Characterization of upconversion nanoparticles

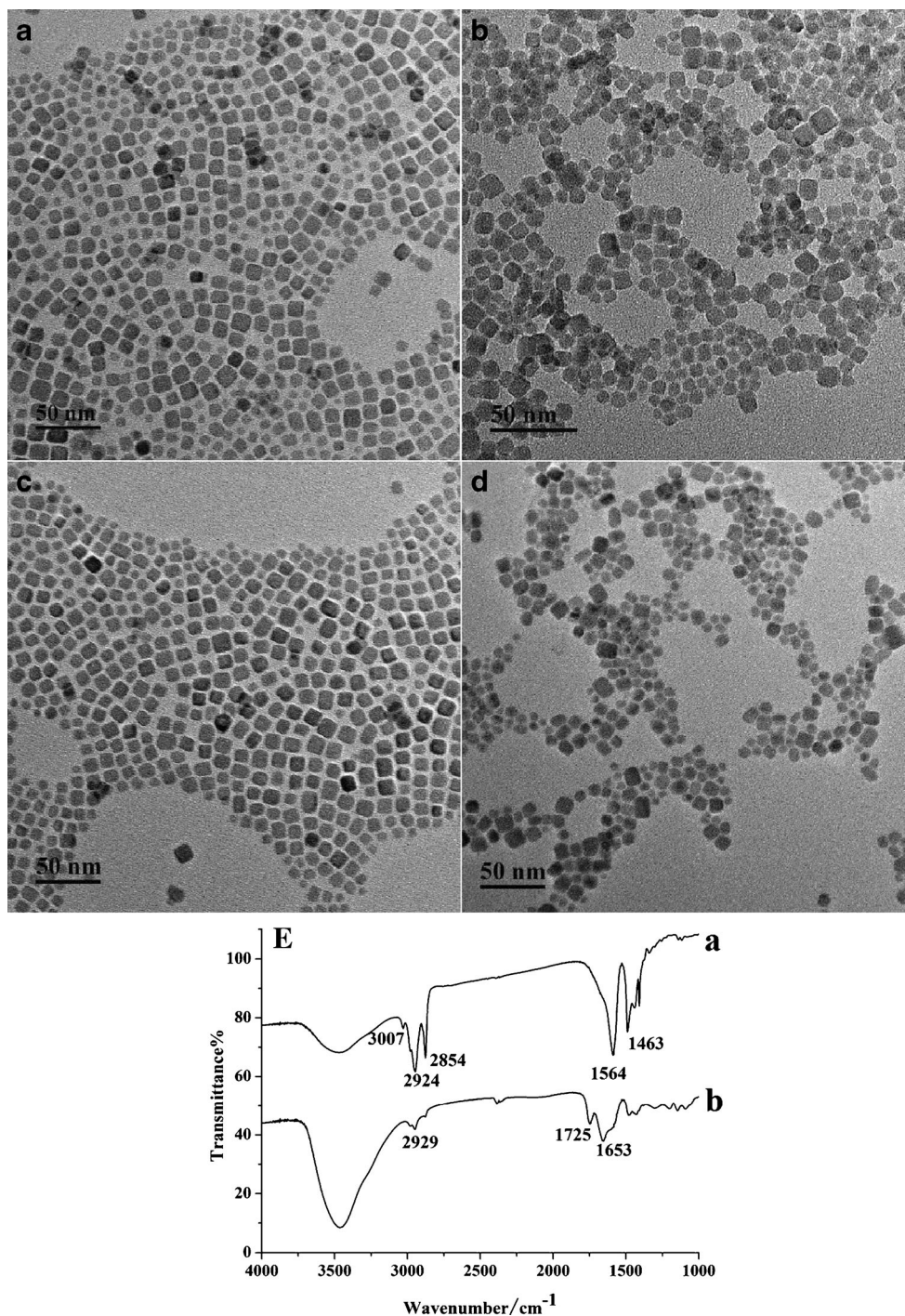
In this work, UCNPs were synthesized by a hydrothermal route in the presence of oleic acid. Figure 2A–D presents

representative TEM images of the oleic acid-capped UCNPs and PAA-capped samples. Due to the presence of oleic acid on the surface of the UCNPs, the oleic acid-capped UCNP sample can only disperse in nonpolar solvents such as cyclohexane, chloroform, and dichloromethane. Therefore, surface functionalization with hydrophilic oleic acid ligand is required prior to the biological applications. Herein, PAA was used as a multidentate ligand to displace the original hydrophobic ligand on the UCNP surface and allow the UCNPs to be dispersed in water. As shown in Fig. 2, the PAA-capped UCNPs still consisted primarily of single nanocubes; however, the formation of nanoarrays was prevented by the carboxylic acid interactions. These observations indicated that the oxidation only affected the UCNP array formation and not their size or shape. The luminescence intensity of the modified samples remained nearly constant.

The ligands capped on the surface of UCNPs were identified by FT-IR spectroscopy, and the results are shown in Fig. 2E. It should be noted that the band at 2924 and 2854 cm⁻¹ in the oleic acid-capped UCNPs corresponded to the asymmetric and symmetric stretching vibrations of the methylene (–CH₂–) in the long alkyl chain. Two strong bands centered at 1564 and 1463 cm⁻¹ were associated with the asymmetric and symmetric stretching vibrations of the carboxylate anions on the surface of the UCNPs before the ligand exchange. A peak at 3007 cm⁻¹ attributed to the =C–H stretching vibration was clearly observed in the spectrum of the as-prepared sample (Fig. 2E curve a). However, in the PAA-capped sample, this feature disappeared after the ligand exchange (Fig. 2E curve b), which suggested a cleavage of the –HC=CH– group. Additionally, the band at around 2929 cm⁻¹ assigned to the asymmetrical stretching of the –CH₂– groups was reduced. Meanwhile, the strong bands at ~1725 and 1653 cm⁻¹ indicated an increase in the quantity of carboxyl groups on the particle surface. Therefore, it was concluded that the surface of UCNPs was modified with PAA.

In the Yb³⁺ and Ho³⁺ co-doped systems, a single green emission at 542 nm was observed in the luminescence spectrum (Fig. 3A). FRET possibly occurred between the NaYF₄: Yb, Ho UCNPs (donor) and the cDNA₁-BHQ₁ (quencher) for which the ultraviolet absorption was approximately at 540 nm. However, we have cited a facile strategy for the rational manipulation of both green and red upconversion emissions, and a pure red emission (660 nm) from NaYF₄: Yb/Er (20/2 mol%) UCNPs was achieved by doping with manganese ions (Mn²⁺) reaching 30 mol% (Fig. 3B). Mn²⁺-doped NaYF₄: Yb/Er nanoparticles were used as an energy donor to cDNA₂-BHQ₃ (quencher) for which the ultraviolet absorption was approximately at 640–670 nm in the FRET protocol. In addition, the green and red emission peaks had large Stokes shifts and could be clearly distinguished from each other. The groups of tunable UCNPs and quenchers were essential to enable simultaneous detection.

Fig. 2 TEM images of oleic acid-capped NaYF₄: Yb, Ho UCNPs (A), NaYF₄: Yb, Er/Mn UCNPs (C), PAA-modified NaYF₄: Yb, Ho UCNPs (B), NaYF₄: Yb, Er/Mn UCNPs (D). FT-IR spectrum of oleic acid-capped NaYF₄ UCNPs (a) and PAA-modified NaYF₄ UCNPs (b) (E)



Characterization of the upconversion nanoparticles conjugated to aptamers

The aptamers were conjugated to the upconversion nanoparticle surfaces through the biotin–avidin affinity reaction. The preparation process included ligand exchange and surface activation, as mentioned above. To verify that the UCNPs were functionalized with aptamers, UV–vis absorption spectroscopy measurements were utilized to monitor the reaction

products, and the results are shown in Fig. 4. First, we can see the strong absorbance of avidin at 280 nm before conjugation to nanoparticles. After carboxy-functionalized nanoparticles were incubated with avidin through EDC/NHS activation, the supernatant was collected. The absorbance of the supernatant liquor was weaker at 280 nm than before functionalization (Fig. 4A). The decrease of peak intensity mainly came from the combination of avidin with carboxy-functionalized nanoparticles. The result also verified that the nanoparticles had

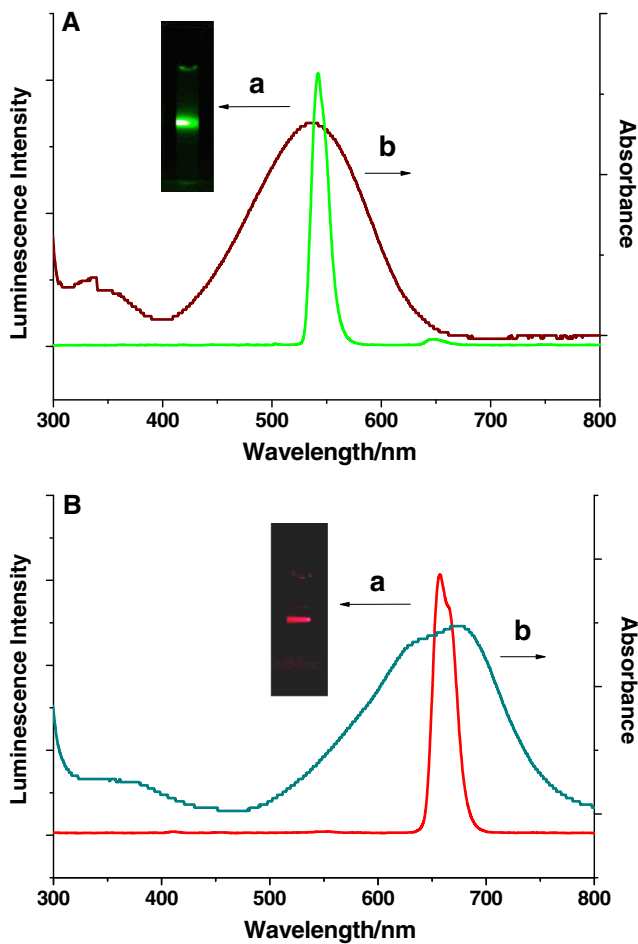


Fig. 3 **A** UV-vis absorption spectra of cDNA₁-BHQ₁ (a) and upconversion luminescence emission spectra of NaYF₄: Yb, Ho UCNPs (b); **B** UV-vis absorption spectra of cDNA₂-BHQ₃ (a) and upconversion luminescence emission spectra of NaYF₄: Yb, Er/Mn UCNPs (b). Photograph of naked-eye-visible green and red upconversion luminescence excited by a 980-nm laser in a transparent aqueous colloid solution

been successfully functionalized with carboxyl groups. Second, for the UV-vis absorbance of aptamers at 260 nm, after the avidin-functionalized UCNPs were incubated with biotinylated aptamers, the absorbance of supernatant aptamers was decreased at 260 nm (Fig. 4B, C). This result indicated that the biotinylated aptamers had been successfully conjugated with UCNPs. Two energy donor probes for corresponding analytes were prepared.

Optimization of the assay conditions

The energy donors and acceptors were very important factors in the FRET system, and the value of the luminescence quencher probes must be evaluated in our approach. To identify the optimal binding concentration for the luminescence quencher probes, a comparative study was performed using a set quantity of luminescence donor probes in the absence of analytes. In detail, various concentrations of the quencher

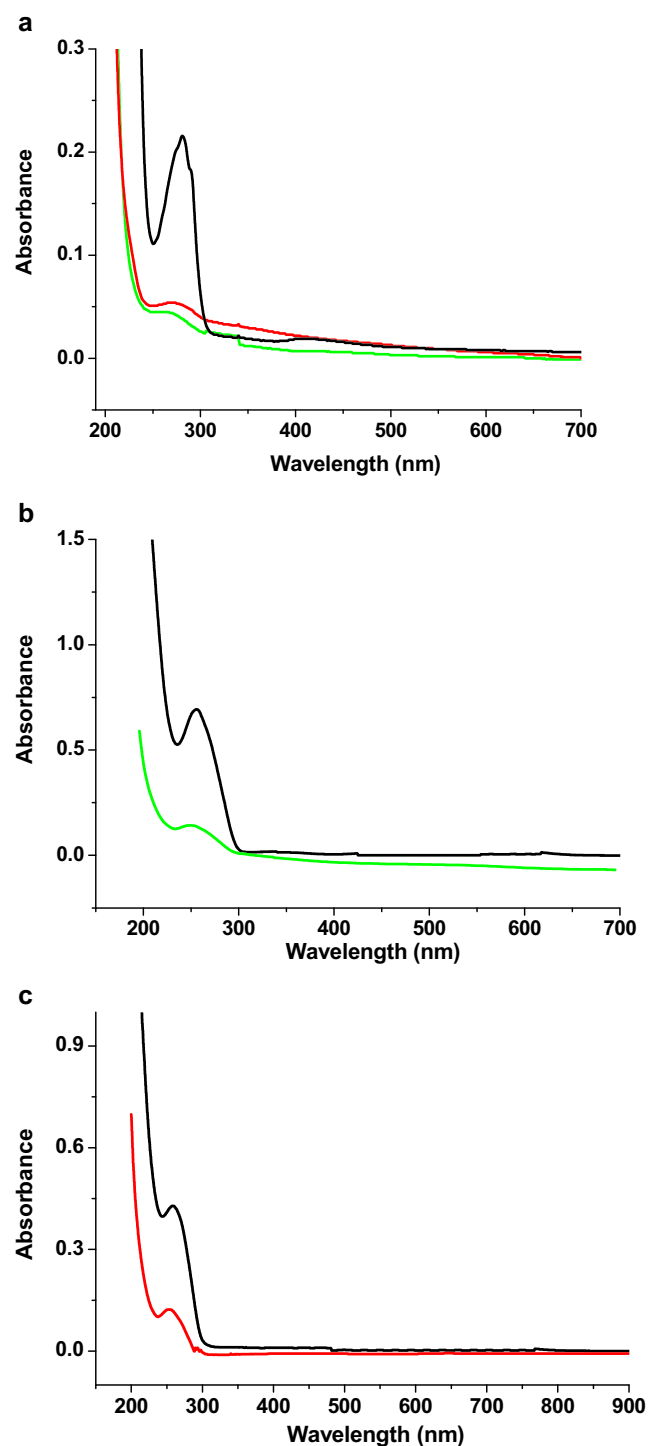


Fig. 4 UV-vis absorption spectra of initial avidin solution (black line in A) and the supernatant liquor after avidin conjugation to NaYF₄: Yb, Ho UCNPs (green line in A), NaYF₄: Yb, Er/Mn UCNPs (red line in A). UV-vis absorption spectra of initial Apt₁ and Apt₂ solution (black line in B and C) and the supernatant liquor after Apt₁ conjugation to NaYF₄: Yb, Ho UCNPs (green line in B) and Apt₂ conjugation to NaYF₄: Yb, Er/Mn UCNPs (red line in C)

probes were hybridized with donor probes in PBS. The luminescence intensity was observed to evaluate the optimization

of the luminescence quencher probes in the FRET system after the hybridization process. Figure 5A (curve a) shows that increasing the cDNA₁-BHQ₁ concentration decreased the green upconversion luminescence intensity. The luminescence of Apt₁-functionalized NaYF₄: Yb, Ho UCNPs reached a steady state when the cDNA₁-BHQ₁ concentration was above 100 μ L. Similarly, the cDNA₂-BHQ₃ concentration decreased the red upconversion luminescence intensity. As a result of Fig. 5A (curve b), 100 μ L cDNA₂-BHQ₃ was employed because of its highly efficient quenching of Apt₂-functionalized NaYF₄: Yb, Er/Mn UCNPs.

In addition, incubation time and incubation temperature were studied. As expected, the luminescence intensity of UCNPs exhibited a gradual decrease with an increasing

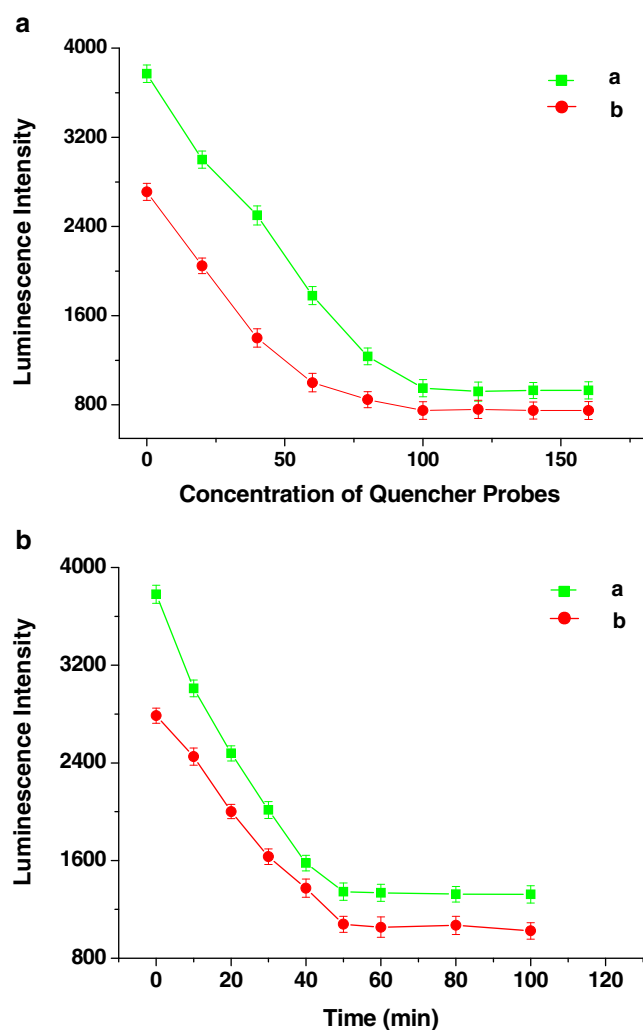


Fig. 5 **A** Luminescence intensity of Apt₁-functionalized NaYF₄: Yb, Ho UCNPs with varying amounts of cDNA₁-BHQ₁ (**a**) and Apt₂-functionalized NaYF₄: Yb, Er/Mn UCNPs with varying amounts of cDNA₂-BHQ₃ (**b**); **B** Effect of incubation time on the luminescence intensity of NaYF₄: Yb, Ho UCNPs (**a**), NaYF₄: Yb, Er/Mn UCNPs (**b**). (The concentration of MC-LR and OA was 0.25 ng mL⁻¹. The illustrated *error bars* represent the standard deviation of seven repeated measurements.)

incubation time. As shown in Fig. 5B, the green and red luminescence reached a steady state after incubation with

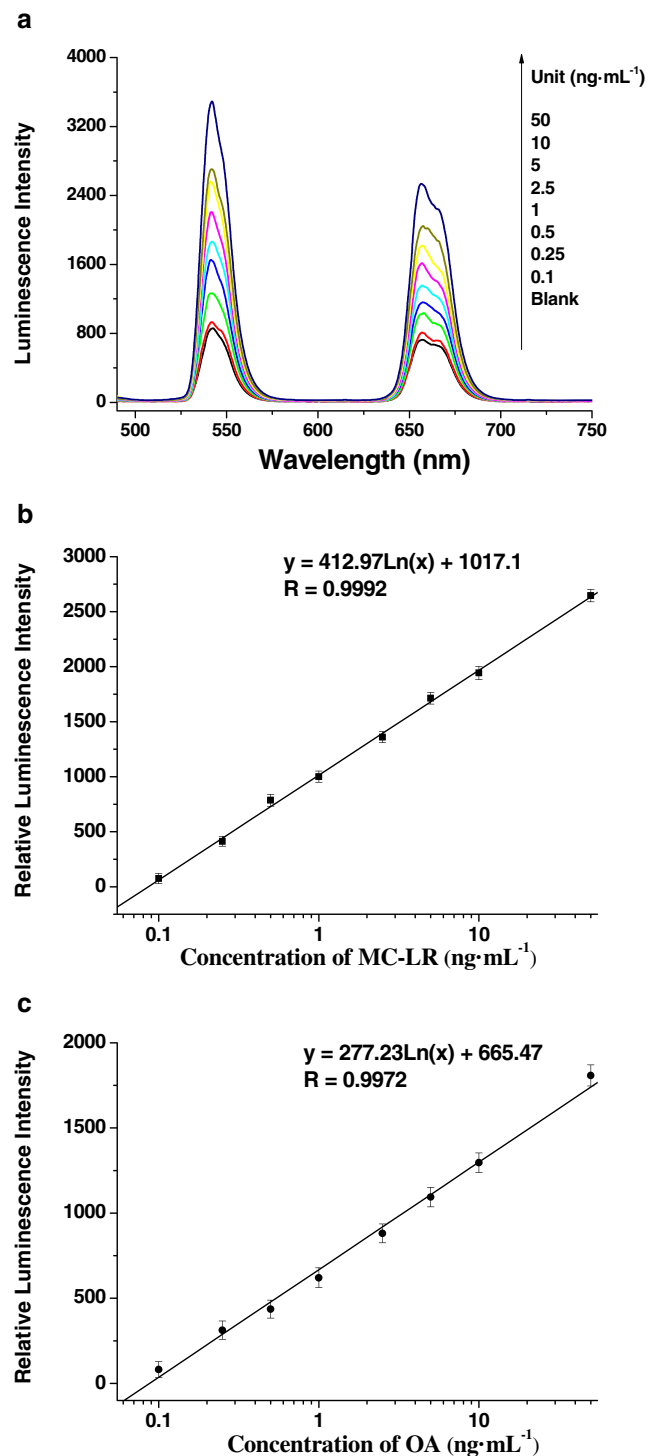


Fig. 6 Typical recording output for the simultaneous detection of different concentrations of MC-LR or OA using the developed method (**A**). Standard curve of the relative luminescence intensity (ΔF) versus the MC-LR concentration (**B**) and OA concentrations (**C**) were measured using the developed method. (The illustrated *error bars* represent the standard deviation of seven measurements conducted at each MC-LR/OA concentration.)

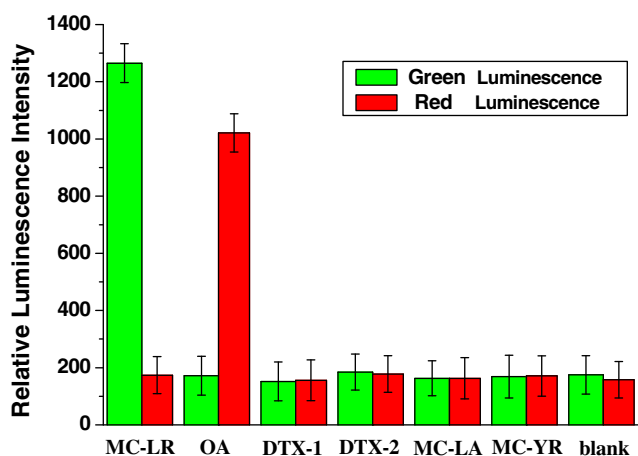


Fig. 7 Selectivity evaluation of the developed method for MC-LR and OA (0.25 ng mL^{-1}) against other analogue (2.5 ng mL^{-1}). (The illustrated error bars represent the standard deviation of seven repeated measurements.)

quencher-labeled cDNA for 50 min. Furthermore, the incubation temperature required for the aptamer recognition of the analytes was based on the literature values and was set at room temperature ($25 \text{ }^\circ\text{C}$).

Quantitative detection of MC-LR and OA

The upconversion luminescence at 542 and 660 nm was chosen to monitor MC-LR and OA, respectively. The detection of MC-LR and OA under optimal conditions was performed, and as the MC-LR and OA concentrations increased, the upconversion luminescence signals gradually increased (Fig. 6A). The toxin concentrations were proportional to the increase in the luminescence intensity (ΔF), where ΔF was

the difference in the upconversion luminescence intensity excited by a 980-nm laser in the absence and presence of MC-LR and OA. The calibration curve of the relationship between the relative intensity of the upconversion luminescence and MC-LR concentration ranged from 0.1 to 50 ng mL^{-1} ($Y=412.97\text{Ln}(x)+1017.1$, $R=0.9992$, Fig. 6B) and from 0.1 to 50 ng mL^{-1} for OA ($Y=277.23\text{Ln}(x)+665.47$, $R=0.9972$, Fig. 6C). Statistical analysis revealed that the detection limits of MC-LR and OA, which were estimated to be 3σ , were 0.025 and 0.05 ng mL^{-1} , respectively. The precision, expressed as the relative standard deviation (RSD) in the MC-LR detection, was equal to 6.47% (10 ng mL^{-1} , $n=7$). The RSD in the OA detection was equal to 6.24% (10 ng mL^{-1} , $n=7$), indicating that the developed method exhibited good reproducibility.

Specificity evaluation for the assay

To test the selectivity of the assay for MC-LR and OA, the effects of other toxins on the dual FRET were evaluated with structures similar to OA, such as dinophysin toxin-1 and 2 (DTX-1, DTX-2), and similar to MC-LR, such as MC-LA and MC-YR. Each type of toxin was added to the prepared detection system individually, and after incubation, the efficiency of the luminescence restoration was recorded. The experimental results shown in Fig. 7 indicate that only MC-LR and OA induced a dramatic luminescence enhancement at their corresponding peaks. None of the other toxins generated significant luminescence signals, even at concentrations ten times greater than that of the target. The results clearly demonstrated this dual FRET assay has high anti-interference capabilities and excellent specificity.

Table 2 Comparison between the developed method and ELISA method for application in water and seafood and recovery results for the spiked MC-LR and OA in real samples using the developed method

Sample	Analyte	Background content (ng mL^{-1})	Added concentration (ng mL^{-1})	ELISA (ng mL^{-1})	Developed method (ng mL^{-1})	Recovery ratio (%)
Water	MC-LR	2.32	0.5	2.77	2.863	108.6
	OA	ND	0.5	0.46	0.513	102.6
	MC-LR	ND	1	0.98	0.991	99.1
	OA	ND	1	1.22	1.201	120.1
Fish	MC-LR	ND	5	5.54	5.114	102.28
	OA	ND	5	5.41	4.987	99.74
	MC-LR	ND	10	11.36	10.324	103.24
	OA	ND	10	9.24	11.421	114.21
Shrimp	MC-LR	ND	5	4.36	5.540	110.8
	OA	ND	5	5.77	4.884	97.68
	MC-LR	ND	25	24.14	26.214	104.86
	OA	ND	25	25.33	25.987	103.95

ND not detected

Analytical applications

The feasibility of applying the dual FRET-based assay to measure MC-LR and OA levels in naturally contaminated samples was validated using six specimens including water, fish, and shrimps. These specimens were measured using our new approach and an available ELISA method. The results in Table 2 showed that there was no significant difference between the methods and that they were highly correlated ($P < 0.0001$). The MC-LR recovery values were between 99.1 and 110.8 %, and the OA recovery values were between 97.68 and 120.1 %, indicating that the developed assay is highly accurate. These analyses demonstrated that the proposed method can be used to detect MC-LR and OA in foodstuff applications.

Conclusions

In summary, this work introduced a novel dual FRET assay that uses UCNP–aptamer ensembles to simultaneously detect MC-LR and OA. This approach exhibited excellent sensitivity and selectivity because of the superior optical features of UCNPs and the high affinity and specificity of the aptamers, which could form aptamer–analyte complexes. Furthermore, two upconversion luminescence peaks, which were excited by a uniform 980-nm laser, acted as donors, and two types of quencher probes were selected to quench the corresponding luminescence. Based on these two donor–acceptor couples, this dual FRET system was built to simultaneously detect MC-LR and OA. This method demonstrated potential for use in practical applications, such as detecting algal and shellfish toxins in the environment and foodstuff, particularly when MC-LR and OA coexist. The platform of this dual FRET system is a promising general optical sensing strategy for the detection of other contaminants in food samples.

Acknowledgments This work was partly supported by NSFC (31401576), JUSRP51309A, the National Science and Technology Support Program of China (2012BAK08B01), NSFC (31401575), the S&T Supporting Project of Jiangsu Province (BE2011621), and the Research Fund for the Doctoral Program of Higher Education (20110093110002).

References

- Carmichael WW (1992) Cyanobacterial secondary metabolites the cyanotoxins. *J Appl Bacteriol* 72:445–459
- Nishiwaki-Matsushima R, Ohta T, Nishiwaki S, Suganuma M, Kohyama K, Ishikawa T, Carmichael WW, Fujiki HJ (1992) Liver-tumor promotion by the cyanobacterial cyclic peptide toxin microcystin-LR. *Cancer Res Clin* 118:420–424
- Suganuma M, Fujiki H, Suguri H, Yoshizawa S, Hirota M, Nakayasu M, Ojika M, Wakamatsu K, Yamada K, Sugimura T (1988) Okadaic acid: an additional non-phorbol-12-tetradecanoate-13-acetate-type tumor promoter. *Proc Natl Acad Sci U S A* 85:1768–1773
- Mestrovic V, Pavela Vrancic A (2003) Inhibition of alkaline phosphatase activity by okadaic acid, a protein phosphatase inhibitor. *Biochimie* 85:647–650
- Dawson RM (1998) The toxicology of microcystins. *Toxicol* 36:953–962
- Bogialli S, Bruno M, Curini R, Di Corcia A, Laganá A, Mari B (2005) Simple assay for analyzing five microcystins and nodularin in fish muscle tissue: hot water extraction followed by liquid chromatography–tandem mass spectrometry. *J Agric Food Chem* 53(17):6586–6592
- Louppis AP, Badeka AV, Katikou P, Paleologos EK, Kontominas MG (2010) Determination of okadaic acid, dinophysistoxin-1 and related esters in Greek mussels using HPLC with fluorometric detection, LC-MS/MS and mouse bioassay. *Toxicol* 55(4):724–733
- Barco M, Rivera J, Caixach J (2002) Analysis of cyanobacterial hepatotoxins in water samples by microbore reversed-phase liquid chromatography–electrospray ionisation mass spectrometry. *J Chromatogr A* 959:103–111
- Suzuki T, Miyazono A, Baba K, Sugawara R, Kamiyama T (2009) LC-MS/MS analysis of okadaic acid analogues and other lipophilic toxins in single-cell isolates of several dinophysis species collected in Hokkaido, Japan. *Harmful Algae* 8(2):233–238
- Yu HW, Lee J, Kim S, Nguyen GH, Kim IS (2009) Electrochemical immunoassay using quantum dot/antibody probe for identification of cyanobacterial hepatotoxin microcystin-LR. *Anal Bioanal Chem* 394(8):2173–2181
- Yu FY, Liu BH, Chou HN, Chu FS (2002) Development of a sensitive ELISA for the determination of microcystins in algae. *J Agric Food Chem* 50(15):4176–4182
- Llamas NM, Stewart L, Fodey T, Higgins HC, Velasco MLR, Botana LM, Elliott CT (2007) Development of a novel immunobiosensor method for the rapid detection of okadaic acid contamination in shellfish extracts. *Anal Bioanal Chem* 389(2):581–587
- Berg K, Wyman J, Carmichael W, Dabholkar A (1988) Isolated rat liver perfusion studies with cyclic heptapeptide toxins of *Microcystis* and *Oscillatoria* (freshwater cyanobacteria). *Toxicol* 26:827–837
- Auzel F (2004) Upconversion and anti-Stokes processes with f and d ions in solids. *Chem Rev* 104:139–173
- Wang F, Banerjee D, Liu YS, Chen XY, Liu XG (2010) Upconversion nanoparticles in biological labeling, imaging, and therapy. *Analyst* 135:1839–1854
- Cheng L, Wang C, Liu Z (2013) Upconversion nanoparticles and their composite nanostructures for biomedical imaging and cancer therapy. *Nanoscale* 5:23–27
- Liu YS, Tu DT, Zhu HM, Chen XY (2013) Lanthanide-doped luminescent nanoprobes: controlled synthesis, optical spectroscopy, and bioapplications. *Chem Soc Rev* 42:6924–6958
- Li ZQ, Zhang Y (2006) Monodisperse silica-coated polyvinylpyrrolidone/NaYF₄ nanocrystals with multicolor upconversion fluorescence emission. *Angew Chem Int Ed* 4:7732–7735
- Wu SJ, Duan N, Shi Z, Fang CC, Wang ZP (2014) Dual fluorescence resonance energy transfer assay between tunable upconversion nanoparticles and controlled gold nanoparticles for the simultaneous detection of Pb²⁺ and Hg²⁺. *Talanta* 128:327–336
- Wu SJ, Duan N, Shi Z, Fang CC, Wang ZP (2014) Simultaneous aptasensor for multiplex pathogenic bacteria detection based on multicolor upconversion nanoparticles labels. *Anal Chem* 86(6):3100–3107
- Wu SJ, Duan N, Ma XY, Xia Y, Wang HG, Wang ZP, Zhang Q (2012) Multiplexed fluorescence resonance energy transfer aptasensor between upconversion nanoparticles and graphene oxide for the simultaneous determination of mycotoxins. *Anal Chem* 84(14):6263–6270

22. Wu SJ, Duan N, Ma XY, Xia Y, Yu Y, Wang ZP, Wang HX (2012) Simultaneous detection of enterovirus 71 and coxsackievirus A16 using dual-colour upconversion luminescent nanoparticles as labels. *Chem Commun* 48(40):4866–4868
23. Wu SJ, Duan N, Zhu CQ, Ma XY, Wang M, Wang ZP (2011) Magnetic nanobead-based immunoassay for the simultaneous detection of aflatoxin B-1 and ochratoxin A using upconversion nanoparticles as multicolor labels. *Biosens Bioelectron* 30(1):35–42
24. Ng A, Chinnappan R, Eissa S, Liu H, Tlili C, Zourob M (2012) Selection, characterization, and biosensing application of high affinity congener-specific microcystin-targeting aptamers. *Environ Sci Technol* 46:10697–10703
25. Eissa S, Ng A, Siaj M, Tavares AC, Zourob M (2013) Selection and identification of DNA aptamers against okadaic acid for biosensing application. *Anal Chem* 85:11794–11801
26. Chen ZG, Chen HL, Hu H, Yu MX, Li FY, Zhang Q, Zhou ZG, Yi T, Huang CH (2008) Versatile synthesis strategy for carboxylic acid-functionalized upconverting nanophosphors as biological labels. *J Am Chem Soc* 130(10):3023–3029
27. Liu CH, Wang H, Li X, Chen DP (2009) Monodisperse, size-tunable and highly efficient β -NaYF₄:Yb, Er (Tm) up-conversion luminescent nanospheres: controllable synthesis and their surface modifications. *J Mater Chem* 19:3546–3553